Effects of Aneurysm on the Mechanical Properties and Histologic Structure of Aortic Sinuses

Eleftherios P. Kritharis, PhD, Dimitrios C. Iliopoulos, MD,
Stavroula A. Papadodima, MD, and Dimitrios P. Sokolis, PhD

Laboratory of Biomechanics, Biomedical Research Foundation of the Academy of Athens; Department of Cardiothoracic Surgery, Athens Medical Center; and Department of Forensic Medicine and Toxicology, Medical School, University of Athens, Athens, Greece

Background. **Aortic root aneurysms are relatively uncommon but their rupture is a detrimental event with acute hemodynamic compromise and high mortality, and there are few available data on their mechanical properties, although aneurysm rupture occurs when hemodynamic stresses exceed wall strength. This study aimed to fill this gap by examining the effect of aneurysm on the mechanical and structural properties of aortic sinuses.**

Methods. **Sinus tissue was procured from 16 aneurysmal patients during surgical repair and from 18 age-matched nonaneurysmal autopsy subjects, and grouped by age (young versus old), region (left versus right versus noncoronary), and direction (circumferential versus longitudinal). The tissue was submitted to histologic evaluation of elastin/collagen contents and to mechanical testing beyond rupture for the determination of failure properties and material characterization by the Fung-type model.**

Results. **Contrasting the direction-dependent (anisotropic) material constants and failure properties, and the primarily circumferential reinforcement of elastin/collagen fibers in healthy sinuses, near-similar (isotropic) properties and arbitrarily aligned fibers were found in the aneurysmal right and left coronary sinuses, together with less anisotropic properties in the aneurysmal noncoronary sinus. Variations between aneurysmal and healthy sinuses were comparable in young and old subjects. The former displayed significantly higher failure stress, failure stretch, and peak elastic modulus, justified by their increased elastin/collagen contents.**

Conclusions. **We submit evidence of more isotropic histomechanical properties in the aneurysmal sinuses that seem consistent with the more axisymmetric stresses exerted on them owing to their more spherical shape, compared with the nondilated healthy sinuses that presented marked anisotropic properties.**

(Ann Thorac Surg 2014;■:■–■)

Aortic root aneurysms are pathologic dilations of the sinuses of Valsalva that appear in less than 1% of open heart surgery patients [1–3], but they can cause aortic insufficiency, dissection, and rupture, carrying high morbidity and mortality [1, 4]. Unlike other aortic aneurysms, they are regularly diagnosed in patients in their second to fourth decades of life, with the risk of dissection/rupture being high even at those young ages and small aneurysm diameters in patients with a family history of aortic dissection or Loyes-Dietz syndrome [5, 6].

The decision to resect an aortic root aneurysm is customarily based on prudent comparison between the risk to the patient of operative intervention and that of fatal rupture if the aneurysm is left unresected. The availability of a criterion for surgical intervention on a patient-specific basis is of utmost importance, and it has been suggested that development of computational stress analyses may assist this aim, serving as a superior clinical tool compared to current recommendations relying largely on the aortic size criterion [7, 8]. Still, necessary inputs to such analyses, namely, the mechanical properties of the aneurysmal sinuses of Valsalva, are very rare [9]. The objective of this study was, consequently, to fill this gap by determining the effect of aneurysm on the histologic structure and mechanical properties of aortic sinus tissue.

Material and Methods

Aortic Sinus Tissue

Unruptured aneurysmal tissue was harvested from 16 consecutive patients (aortic diameter, 5.3 ± 1.5 cm) undergoing surgical repair at the Department of Cardiothoracic Surgery of Athens Medical Center. Whole nonaneurysmal sinuses (control) were procured within 24 hours of death from 18 subjects during autopsy at the Department of Forensic Medicine and Toxicology of the University of Athens Medical School. The research protocol was approved by the Institutional Ethics Committee on Human Research under informed consent from the patients and from relatives for the cadaveric subjects. Patient data were obtained from hospital charts and cadaveric data during autopsy (Table 1). The sinuses were cleansed in refrigerated saline, and periadventitial tissues were removed. Histologic processing and mechanical studies took place within 24 hours after resection.

Accepted for publication March 13, 2014.

Address correspondence to Dr Sokolis, 35 Lefkados St, Athens 15354, Greece; e-mail: dimitrissokolis@ath.forthnet.gr.

Published by Elsevier Inc

0003-4975/$36.00
http://dx.doi.org/10.1016/j.athoracsur.2014.03.016

Table 1. Preoperative Patient and Autopsy Characteristics

	Age (Years)	Sex	Diameter (cm)	Risk Factors and Comorbidities	Valve Type	Valve Function
Patient no.						
1	82	Male	5.9	HT, diabetes, smoking	TAV	R/S
2	82	Female	5.2	Smoking, obesity, ATAA	TAV	R
3	27	Male	4.5	Smoking, Marfan, ATAA	TAV	Normal
4	67	Male	6.6	HT, smoking, CAD, hyperlipidemia	TAV	R
5	49	Male	5.5	HT, smoking, ATAA	TAV	R
6	81	Male	5.1	HT, CAD	TAV	R/S
7	64	Female	4.7	Diabetes, ATAA	TAV	R/S
8	53	Female	4.5	HT, obesity, ATAA	TAV	R
9	19	Male	5.0	Obesity, Marfan	TAV	R
10	72	Male	5.2	HT, diabetes, CAD, smoking	TAV	R
11	46	Male	5.5	HT	BAV	R
12	31	Male	4.9	Marfan	TAV	R
13	37	Male	6.1	Smoking	BAV	R
14	65	Male	5.3	HF, HT, ATAA	TAV	R
15	61	Male	5.5	HT, diabetes, CAD	TAV	R
16	67	Male	5.6	HT, smoking, mitral valve prosthesis	TAV	R
Autopsy no.						
1	54	Male	…	HT, CAD, diabetes	TAV	…
2	52	Male	…	None	TAV	…
3	54	Female	…	None	TAV	…
4	51	Male	…	HT, CAD	TAV	…
5	50	Male	…	None	TAV	…
6	74	Male	…	HT	TAV	…
7	66	Male	…	Smoking	TAV	…
8	81	Male	…	HT	TAV	…
9	80	Male	…	None	TAV	…
10	80	Male	…	HT	TAV	…
11	72	Male	…	Smoking, CAD	TAV	…
12	57	Male	…	Smoking, CAD	TAV	…
13	39	Male	…	None	TAV	…
14	56	Male	…	HT, smoking	TAV	…
15	47	Female	…	Smoking	TAV	…
16	43	Male	…	None	TAV	…
17	16	Female	…	None	TAV	…
18	39	Male	…	None	TAV	…

Maximum aneurysm diameter as evaluated from preoperative computed tomography, magnetic resonance imaging, or echocardiography examination. Blank entry indicates nonaccessible parameter.

ATAA = ascending thoracic aortic aneurysm; BAV = bicuspid aortic valve; CAD = coronary artery disease; HF = heart failure; HT = hypertension; R = regurgitation; S = stenosis; TAV = tricuspid aortic valve.

Quantitative Histology

Sinus specimens (one per subject and sinus), adjacent to those kept for mechanical testing, were fixed over 24 hours with formalin and embedded in paraffin. Sections, 5 μm thick, with circumferential (CIRC) and longitudinal (LONG) direction were cut and treated with hematoxylin-eosin for nucleus, orcein for elastin, and sirius red for collagen differentiation. As previously [9, 10], digitized polychromatic images were acquired by an Altra20 camera (Soft Imaging System GmbH, Münster, Germany) fitted to a light microscope (Olympus CX31; Olympus, Tokyo, Japan), and processed semiautomatically with Image-Pro Plus, version 4.5, software (Media Cybernetics, Silver Spring, MD). Elastin and collagen area densities (considered as contents) of the entire wall were blindly assessed in 10 representative positions after micrograph segmentation and averaged in three sections.

Mechanical Testing

Rectangular strips were excised from each sinus in the CIRC and LONG directions, and cut into dumbbell shape, having 3-mm-long by 3-mm-wide ends and a middle effective section 7 mm long by 2 mm wide. The ends of each strip were mounted into the grips of a Vitrodyne V1000 Universal Tester (Liveco, Burlington, VT) and mechanically analyzed, as reported by our group

[9–11]. The strip's original thickness and width were measured in triplicate by a laser micrometer (LS-3100; Keyence Corp, Osaka, Japan); its original (effective) length established by adjusting the distance between grips to record zero tensile load and checked by the lack of tissue folding. In the course of testing, strip and grips were immersed in saline solution at 37°C. An actuator moved the upper grip away from the lower at 100 μm/s, elongating each strip beyond rupture, during which elongation in its effective section was monitored by piezoelectric crystals (Sonometrics Corp, London, Ontario, Canada), glued on the intimal aspect of tissue (Fig 1), and the uniaxial load exerted was recorded by a load cell (GSO-500; Transducer Techniques, Temecula, CA). Tests were retained for evaluation if rupture occurred away from the grips. Most strips ruptured twice, with the inner layers failing before the outer.

Analysis

From the load-elongation data, stress-stretch curves were plotted. Stretch was our preferred deformation metric, because it is most convenient to track experimentally, defined as the elongated over the original length of strip. The Cauchy definition, namely, load times stretch over the original cross-sectional area, was our preferred stress metric, because it represents the true intensity of stress experienced by the tissue, therefore being most relevant in failure considerations. Failure stress and stretch, considered as metrics of the full capacity of tissue to sustain stress and of its extensibility, in turn, were computed as stress and stretch at the initial failure of sinus tissue. Peak elastic modulus, a metric of the maximum stiffness of tissue (ie, of its full resistance to deformation in response to applied stress), was the highest gradient of the stress-stretch curve before the initial failure.

The stress-stretch curves were fitted by the exponential Fung-type material model [12]:

$$W = K(e^{Q} - 1), \quad Q = c_{\theta\theta}E_\theta^2 + c_{zz}E_z^2 + c_{\theta z}E_\theta E_z\,,$$

hypothesizing that sinus tissue is a homogeneous and anisotropic (with different properties in the CIRC and LONG directions) membrane subject to finite, pseudoelastic (ie, hyperelastic during loading), and isovolumetric elongations, as commonly done for cardiovascular tissues. (For extensive discussion of these hypotheses, reference is made to Fung [12].) In the equation above, $E_i = 1/2(\lambda_i^2 - 1)$, $i=\theta,z$ were CIRC and LONG Green strains, expressed by stretches λ_θ and λ_z. Material constants $c_{\theta\theta}$, c_{zz}, and $c_{\theta z}$ specified CIRC stiffness, LONG stiffness, and stiffness interaction among axes; and constant K served as scaling factor, so that the higher the values of the remaining constants, the smaller its value would be. Principal stresses σ_θ and σ_z were defined as $\sigma_i = \lambda_i \partial W/\partial\lambda_i$.

Material constants were determined using the Levenberg-Marquardt least-squares algorithm in MicroCal Origin, version 7.5 (OriginLab Corp, Northampton, MA). Physically realistic values of those constants were ensured by restraining them with thermodynamic inequalities valid for anisotropic membranes [13]. The quality of fitting was evaluated by root-mean-square error ε and determination coefficient r^2, as previously [9].

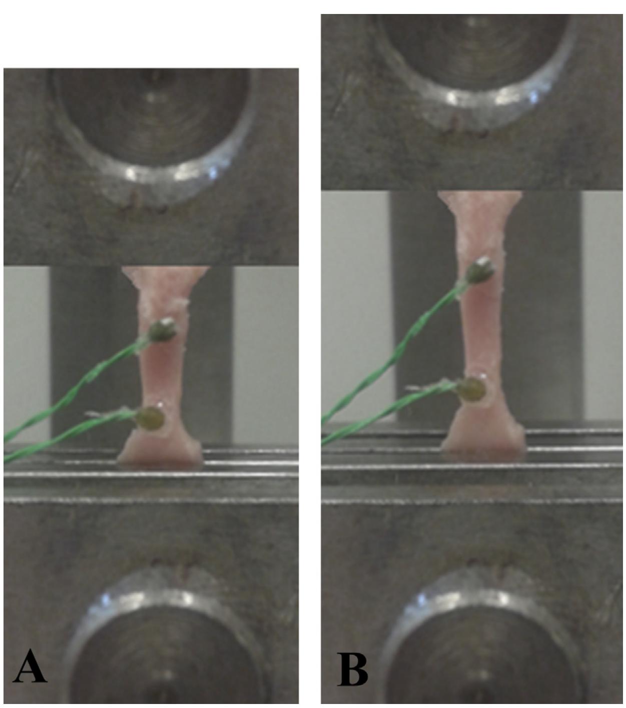

Fig 1. Close-view photographs of a typical sinus specimen under (A) zero load and (B) moderate load, while mounted into the grips of the uniaxial tensile tester. Shown also are the piezoelectric crystals glued on the specimen's middle section for monitoring its elongation during testing.

Statistics

Results are expressed as mean ± SE. Regional, pathologic, and age differences were identified by three-way analysis of variance and Tukey test, and directional differences with Student's t test. The Spearman rank correlation was used to describe associations between different variables. Statistical significance was set at p value less than 0.05.

Results

Nonsignificant were the age differences (young subjects [<45 years], 29 ± 4 versus 34 ± 6 years, $p > 0.2$; old subjects, 66 ± 4 versus 62 ± 3 years, $p > 0.2$) between patients undergoing surgery and autopsy subjects. The results from 13 patients were reported earlier [9]. Aneurysmal sinuses were thinner than control in both young and old subjects (Fig 2).

Figure 3 shows typical stress-stretch curves of aneurysmal and control sinuses from young and old subjects, displaying an exponential shape that was fit closely ($r^2 > 0.95$) by the Fung-type model through material constant values listed in Table 2. The failure properties of aneurysmal tissue were similar to those of control in the noncoronary sinus (NCS) in either direction or age group, *Fig 2. No-load thickness of fresh tissue from aneurysmal subjects (black bars) and control subjects (gray bars) for (A) young group and (B) old group. †‡Significant differences against control and old, respectively. Inside parentheses are the number of specimens used for thickness measurement. (LCS = left coronary sinus; NCS = noncoronary sinus; RCS = right coronary sinus.)*

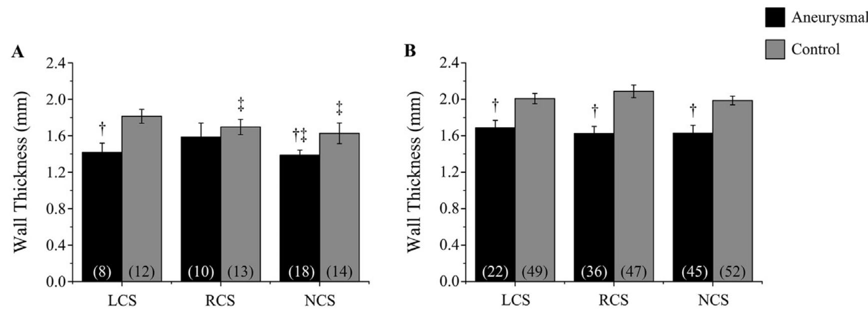

whereas in the other sinuses of older subjects, failure stress and peak elastic modulus of aneurysmal tissue were smaller in the CIRC but greater in the LONG axis (Fig 4), and material constants were essentially nonvarying compared with control.

Elastin/collagen contents did not differ notably between aneurysmal and control sinuses, but invariably declined with age (Fig 5). Collagen content correlated positively with failure stress ($r = 0.67$, $p < 0.001$) and peak elastic modulus ($r = 0.60$, $p < 0.001$), as did elastin content with failure stretch ($r = 0.49$, $p < 0.001$) and stress ($r = 0.45$, $p < 0.001$). Correlations between aneurysm diameter and all failure parameters were negative but weak ($r > -0.3$).

Comment

Consideration of Findings

The major finding of this study was that aneurysmal tissue showed less obvious directional differences in NCS, and near-similar stress-stretch curves, material constants, and failure properties in the right coronary sinus (RCS) and left coronary sinus (LCS) (Figs 3 and 4, Table 2), contrasting the direction-dependent properties in all healthy sinuses. Importantly, this mechanical adaptation seems to correlate with the histologic adaptation noted in those sinuses. Particularly, we observed that the aneurysmal RCS and LCS, and to a lesser extent the NCS, exhibited a complex microstructural organization with arbitrarily aligned lamellar units (Figs 6 and 7). The microstructure was more homogeneous in nonaneurysmal sinuses, albeit not to the extent of the ascending aorta, comprising elastic laminae, collagen bundles, and smooth muscle cells, all with uniform CIRC alignment [8]. Consideration of stresses in the sinus wall taken as a thin-walled structure (Laplace's law) offers an explanation for this histomechanical adaptation of aneurysmal sinuses. Their isotropic properties are consistent with the more axisymmetric stresses (ie, the ratio of stresses in the CIRC and LONG axes is close to 1:1) exerted on them because of their more spherical shape, and so are the anisotropic (direction-dependent) properties of healthy sinuses with their nondilated bulb-shaped geometry, for which the stress ratio is between 1:1 and 1:2.

The age-related differences in mechanical properties were similar for both aneurysmal and control tissue, with the younger specimens presenting greater tensile strength and maximum tissue stiffness (Fig 4) along with greater extensibility (data not shown), justified by their higher elastin and collagen contents (Fig 5). These results

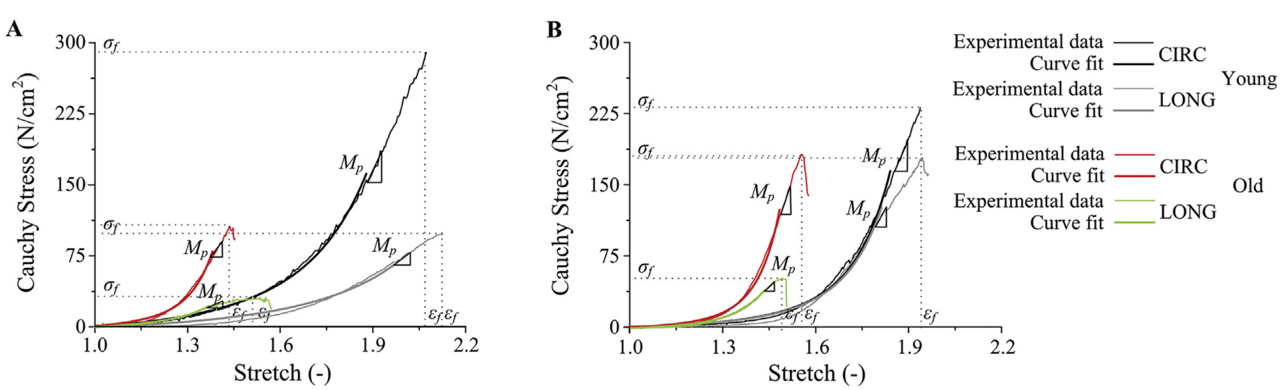

Fig 3. Typical Cauchy stress-stretch curves of (A) aneurysmal specimens and (B) control specimens in the circumferential (CIRC) and longitudinal (LONG) directions derived from the noncoronary sinus (NCS) of young and old subjects. Failure stress (σ_f) and stretch (ε_f) are marked with dotted lines, and peak elastic modulus (M_p) is marked with a triangle denoting slope. Fung-type model predictions are plotted with thick lines. (Thin black lines = experimental data CIRC young; thick black lines = curve fit CIRC young; thin gray lines = experimental data LONG young; thick gray lines = curve fit LONG young; thin red lines = experimental data CIRC old; thick red lines = curve fit CIRC old; thin green lines = experimental data LONG old; thick green lines = curve fit LONG old.)

Table 2. Material Constants and Fitting Quality of Fung-Type Model for Aneurysmal and Control Specimens Categorized by Age and Region

Variable	Region	K (N/cm^2)	$c_{\theta\theta}$ (–)	c_{zz} (–)	$c_{\theta z}$ (–)	ε (N/cm^2)	r^2 (–)
Young							
Aneurysmal	LCS (n = 4)	4.152 ± 1.088[a]	1.961 ± 0.583[a]	1.880 ± 0.739[a]	1.073 ± 0.502[a]	3.674 ± 0.599	0.996 ± 0.001
	RCS (n = 5)	6.749 ± 2.418	1.415 ± 0.673[a]	1.975 ± 0.808[a]	1.059 ± 0.471[a]	3.817 ± 1.238	0.990 ± 0.004
	NCS (n = 8)	4.125 ± 0.655[a]	2.106 ± 0.277[a,b]	1.789 ± 0.249[a]	1.131 ± 0.252[a]	3.248 ± 0.831	0.993 ± 0.003
Control	LCS (n = 6)	4.488 ± 1.141[a]	1.308 ± 0.187[a]	1.408 ± 0.243[a]	1.114 ± 0.148[a]	9.593 ± 2.682	0.989 ± 0.003
	RCS (n = 6)	5.931 ± 2.102[a]	1.832 ± 0.574[a]	1.593 ± 0.455[a]	1.174 ± 0.359[a]	13.447 ± 4.308	0.978 ± 0.009
	NCS (n = 6)	3.990 ± 1.027[a]	1.871 ± 0.343[a]	1.949 ± 0.480[a]	1.270 ± 0.373[a]	15.514 ± 3.114	0.981 ± 0.005
Old							
Aneurysmal	LCS (n = 9)	1.710 ± 0.419	5.218 ± 0.801[c]	4.959 ± 1.102	3.082 ± 0.546	5.650 ± 1.365	0.978 ± 0.008
	RCS (n = 18)	2.194 ± 0.372	7.558 ± 1.418	5.228 ± 1.067	3.997 ± 1.016	4.985 ± 1.187	0.985 ± 0.003
	NCS (n = 20)	1.150 ± 0.143	7.753 ± 1.332[b]	5.290 ± 0.573	3.978 ± 0.800	4.356 ± 0.861	0.988 ± 0.003
Control	LCS (n = 22)	1.892 ± 0.411	9.063 ± 1.418[b]	5.875 ± 1.484	4.063 ± 0.727	5.650 ± 1.365	0.986 ± 0.002
	RCS (n = 23)	1.925 ± 0.367	7.879 ± 1.224[b]	4.862 ± 1.008	3.890 ± 0.625	7.822 ± 0.897	0.988 ± 0.002
	NCS (n = 23)	1.493 ± 0.245	10.088 ± 1.864[b]	6.105 ± 0.978	5.243 ± 1.318	10.372 ± 1.523	0.972 ± 0.009

[a] $p < 0.05$ against old. [b] $p < 0.05$ against c_{zz}. [c] $p < 0.05$ against control.

Number (n) indicates number of strip pairs.

LCS = left coronary sinus; NCS = noncoronary sinus; RCS = right coronary sinus.

highlight the importance of using age-matched sinus tissues when considering differences between dilated and nondilated sinuses. We have earlier demonstrated that ascending aortic aneurysms are not associated with wall weakening [10]. Herein, the failure properties of NCS did not vary among aneurysmal and age-matched control

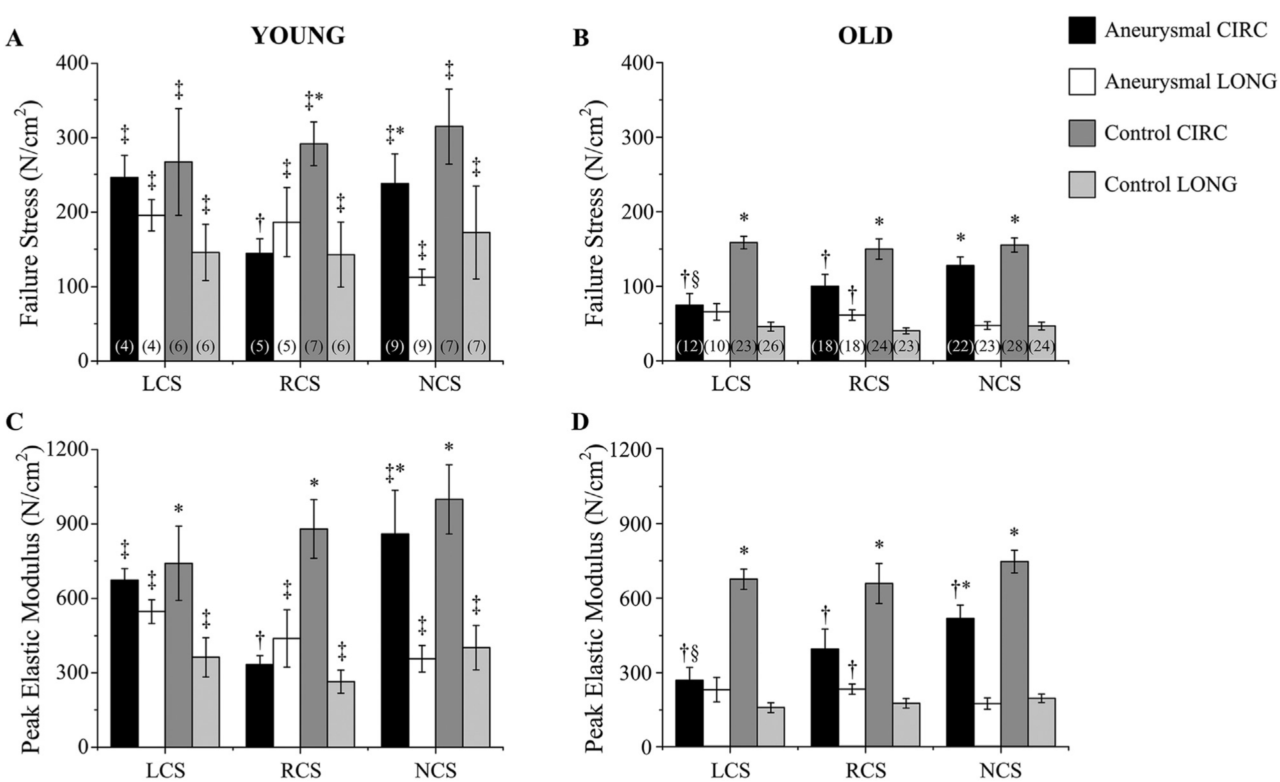

Fig 4. (A, B) Failure stress and (C, D) peak elastic modulus of aneurysmal and control specimens from the left coronary sinus (LCS), right coronary sinus (RCS), and noncoronary sinus (NCS). Specimens are further categorized as young and old. †‡§Significant differences against control, old, longitudinal (LONG), and NCS, respectively. Inside parentheses are the number of specimens used for determining failure properties. (Black bars = aneurysmal CIRC; white bars = aneurysmal LONG; dark gray bars = control CIRC; light gray bars = control LONG.)*

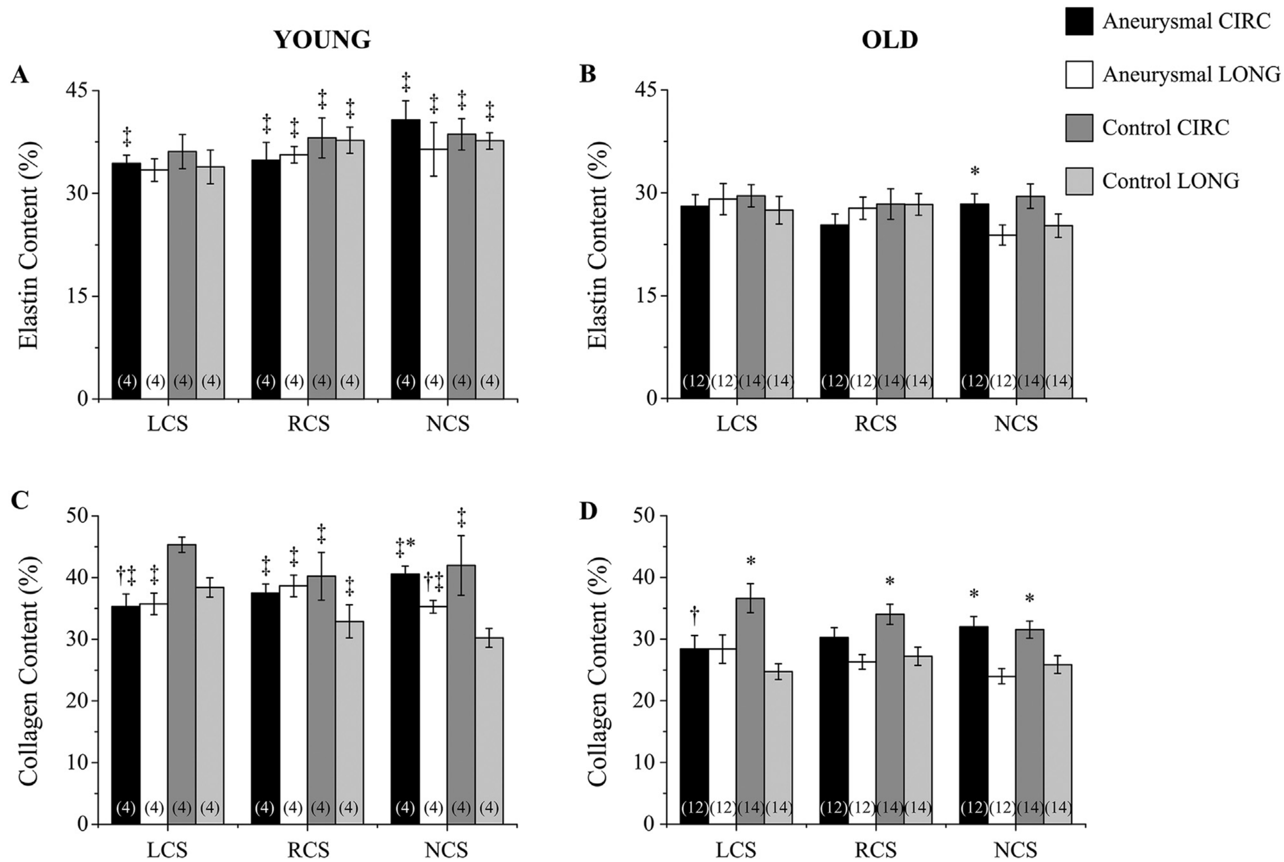

*Fig 5. (A, B) Elastin and (C, D) collagen contents in the entire wall of circumferential (CIRC) and longitudinal (LONG) left coronary sinus (LCS), right coronary sinus (RCS), and noncoronary sinus (NCS) sections from aneurysmal and control subjects for young and old subjects. †‡*Significant differences against control, old, and LONG specimens, respectively. Inside parentheses are the number of specimens used for content measurements. (Black bars = aneurysmal CIRC; white bars = aneurysmal LONG; dark gray bars = control CIRC; light gray bars = control LONG.)*

tissue. In LCS and RCS, aneurysmal tissue showed increased tensile strength and maximum stiffness longitudinally and decreased properties circumferentially, yet this was not due to a supposedly degenerative effect on tissue, but rather by virtue of the change in anisotropy caused by the adapted histology of tissue. In accordance with the present results, we recently found that failure stress and stretch were negatively correlated with age [9]. Unlike wall stiffness at high loads, specified by peak elastic modulus, which decreased with aging, material constants $c_{\theta\theta}$, c_{zz}, and $c_{\theta z}$, specifying stiffness at physiologic loads, increased (Table 2), with unfavorable implications for the function and longevity of the aortic leaflets [14]. The regional dependence of the material constants and failure properties of aneurysmal tissue may be related to their specialized structure and failure modes; for example, the sinus with smallest strength may be more prone to rupture than the other sinuses orthogonally to the direction of smallest strength.

Comparison with Previous Studies

Except for our recent study [9], data in the literature pertain to the passive properties of nondilated human sinus tissue without histologic or other quantification of elastin/collagen contents. Early studies involved the uniaxial stress-strain relationship of CIRC and LONG strips from porcine tissue [15–17], but these were confined by the limited sample sizes; and no systematic comparisons with age, region, and direction were performed. Recent studies reporting on the biaxial stress-strain relationship provide valuable data; then again, failure properties are missing although biomechanical analysis of the rupture modes of aortic root aneurysms mandates a full set of data describing also those properties. Among the studies investigating human tissue, nonsignificant stiffness differences among sinuses in either direction have been unanimously reported [18, 19], suggestive of no regional dependence in the mechanical response as we have found for control tissue in either age group. Still, there were differing opinions on issues of directional dependence, namely, of anisotropic behavior, with one study [19] disclosing no difference in stiffness at 120 kPa stress between the CIRC and LONG axes in all three sinuses, unlike the other [18], which demonstrated higher CIRC than LONG stiffness at 60 kPa stress in every sinus, in good agreement with our data.

A reduced thickness of aneurysmal versus control tissue was confirmed on fresh tissue. Both tissues became thicker in older individuals, yet we disclose that thickness

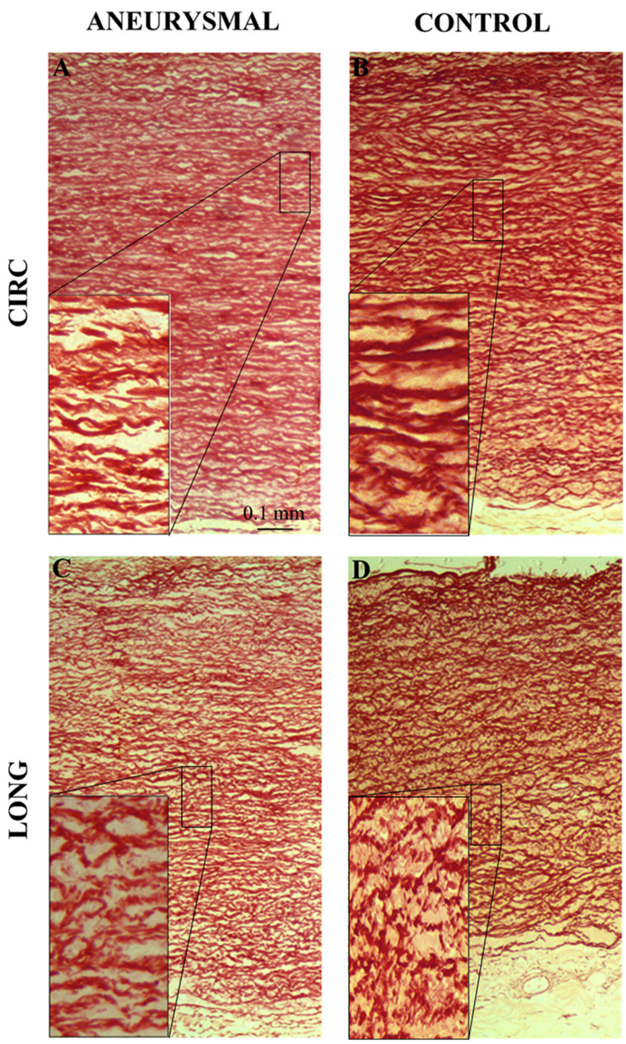

Fig 6. Orcein-stained sections from the aneurysmal (left) and control (right) right coronary sinus of old subjects. (A, B) Circumferential (CIRC) sections. (C, D) Longitudinal (LONG) sections. Magnification is ×10, with higher magnification (×40) of the rectangular region shown in the insets.

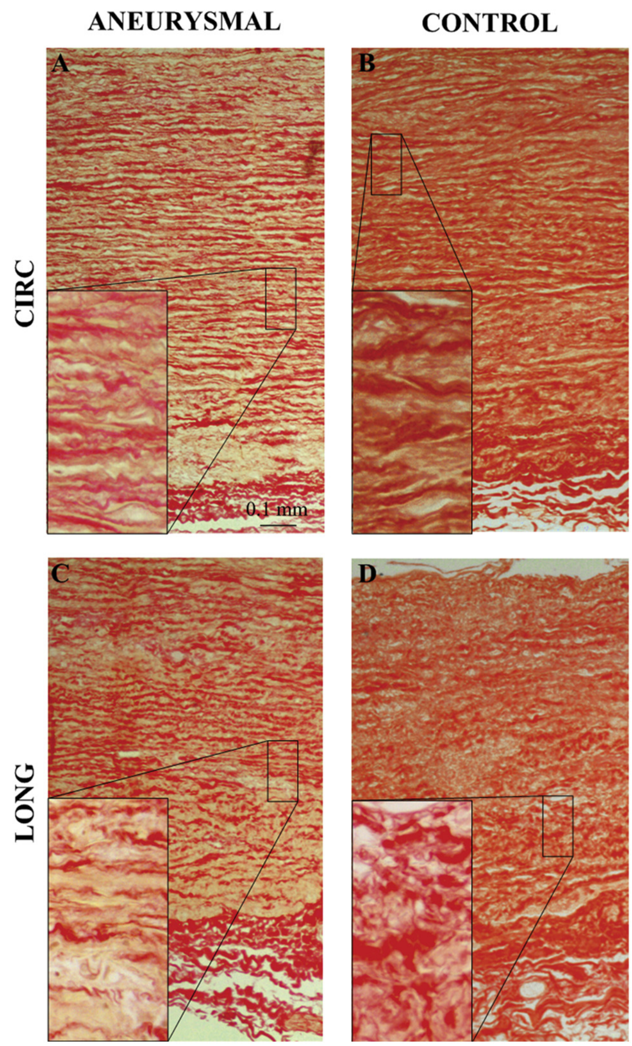

Fig 7. Sirius-red-stained sections from the aneurysmal (left) and control (right) right coronary sinus of old subjects. (A, B) Circumferential (CIRC) sections. (C, D) Longitudinal (LONG) sections. Magnification is ×10, with higher magnification (×40) of the rectangular region shown in the insets.

was regionally invariant (Fig 2), as in [18, 19] for nondilated sinuses. Our stress-stretch data showed for both aneurysmal and control tissue that stresses in both axes increased exponentially with increasing strains (Fig 3), consistent with studies on nondilated tissue [18, 19] implementing also the Fung-type model.

Clinical Implications

Knowing the mechanical properties of Valsalva sinuses is of major functional importance and is needed for understanding the modes of rupture and dissection of aortic root aneurysms, which represent structural failures of the aortic root wall arising when hemodynamic stresses overcome the tissue's ability to sustain stress. Aneurysm size continues to be the most common clinical metric used for predicting the rupture potential. The mechanical properties of wall tissue are equally important determinants of wall stress from the biomechanics viewpoint, but there has been no prior attempt to correlate the rupture potential with specific mechanical properties. A better assessment of stresses in sinus of Valsalva aneurysms, rather than by invoking Laplace's law, will permit a better prediction of aneurysms that are likely to rupture and require immediate intervention. Such a decision will be aided by computational analyses, accounting for the patient-specific geometry and wall mechanics. Such analyses might also optimize aortic valve-sparing operations in patients with sinus of Valsalva aneurysms [4] by restoring physiologic root properties and anatomy of the native and synthetic root components, thereby preventing valvular damage and obtaining adequate valvular function. To that purpose, our study describes and validates numerically a material model that consistently characterizes the mechanical response of healthy sinus tissue, age-matched with the replaced aneurysmal tissue, to be employed in computational studies that model valve-sparing operations, as previous studies have used unrealistic tissue properties [20].

Study Limitations

There are several limitations to our study. Those pertaining to the experimental protocols used for mechanical testing and the model used for material characterization have been previously discussed [9], along with those pertaining to the nonconsideration of sinus wall heterogeneity, namely, the determination of layer-specific properties. The results presented herein must also be interpreted with caution regarding sinus function in the living human, as the stresses and strains applied were under in vitro experimental conditions of uniaxial tension and with surrounding tissues dissected. Excess tissue, however, from the aneurysmal RCS and LCS was not usually available in the quantity needed for biaxial testing methods that would permit a more physiologically relevant characterization of material constants. Even so, uniaxial testing allowed the determination of rupture properties, which is not possible with biaxial tension because of tissue tearing by the sutures used for attachment. We have further hypothesized that the no-load state of aortic sinus tissue was its zero-stress state. Knowing the true zero-stress state is vital for mechanical analysis, serving as the reference state for computing stresses and strains. Another issue to consider was the small study population, forbidding classification of patients by sex, presence of Marfan's syndrome or bicuspid aortic valve, valvular hemodynamic abnormality (ie, aortic stenosis, aortic insufficiency, or combined). Future studies could address the effects of these clinical factors and also compare the histomechanical properties of tissue from patients having aneurysm rupture with those from patients receiving elective repair. Such data could offer much-needed insight into the biomechanical mechanisms governing aneurysm rupture by elucidating whether ruptured tissue is actually more vulnerable to rupture when exposed to identical hemodynamic loads, by being weaker or stiffer compared with unruptured tissue.

To conclude, histologic and mechanical differences between aneurysmal and control sinus tissue were detected, according to age, region, and direction. Such data have physiologic and clinical relevance because the mechanical properties determine the wall stresses generated on aortic sinuses, and the failure properties determine the resistance to rupture. With the current material model and the associated material constants, the distributions of physical stresses and strains may be evaluated under in vivo conditions, and the function of dilated and age-matched healthy aortic sinuses may be studied from the engineering standpoint using the analytical methods of continuum mechanics. This information will broaden our fundamental understanding of aortic sinus remodeling with aneurysm formation and aid the task of developing more suitable diagnostic tools for surgical intervention.

The authors thank Vasiliki Androutsopoulou, MD, for assistance with the acquisition of patient preoperative data.

References

1. Takach TJ, Reul GJ, Duncan JM, et al. Sinus of Valsalva aneurysm or fistula: management and outcome. Ann Thorac Surg 1999;68:1573–7.
2. Heydorn WH, Nelson WP, Fitterer JD, et al. Congenital aneurysm of the sinus of Valsalva protruding into the left ventricle: review of diagnosis and treatment of the non-ruptured aneurysm. J Thorac Cardiovasc Surg 1976;71:839–45.
3. Chu SH, Hung CR, How SS, et al. Ruptured aneurysms of the sinus of Valsalva in oriental patients. J Thorac Cardiovasc Surg 1990;99:288–98.
4. David TE. Surgical treatment of ascending aorta and aortic root aneurysms. Prog Cardiovasc Dis 2010;52:438–44.
5. Williams JA, Loeys BL, Nwakanma LU, et al. Early surgical experience with Loeys-Dietz: a new syndrome of aggressive thoracic aortic aneurysm disease. Ann Thorac Surg 2007;83:757–63.
6. Yacoub MH, Gehle P, Chandrasekaran V, et al. Late results of a valve-preserving operation in patients with aneurysms of the aorta and root. J Thorac Cardiovasc Surg 1998;115:1080–9.
7. Phillippi JA, Pasta S, Vorp DA. Biomechanics and pathobiology of aortic aneurysms. In: Studies in mechanobiology, tissue engineering and biomaterials. Vol 7. Berlin: Springer-Verlag; 2011:67–118.
8. Sokolis DP, Kritharis EP, Giagini AT, Lampropoulos KM, Papadodima SA, Iliopoulos DC. Biomechanical response of ascending thoracic aortic aneurysms: association with structural remodeling. Comput Meth Biomech Biomed Eng 2012;15:231–48.
9. Iliopoulos DC, Kritharis EP, Boussias S, Demis A, Iliopoulos CD, Sokolis DP. Biomechanical properties and histological structure of sinus of Valsalva aneurysms in relation to age and region. J Biomech 2013;46:931–40.
10. Iliopoulos DC, Kritharis EP, Giagini AT, Papadodima S, Sokolis DP. Ascending thoracic aortic aneurysm is associated with vessel stiffening and compositional remodeling but not weakening in age-matched subjects. J Thorac Cardiovasc Surg 2009;137:101–9.
11. Iliopoulos DC, Deveja RP, Kritharis EP, et al. Regional and directional variations in the mechanical properties of ascending thoracic aortic aneurysms. Med Eng Phys 2009;31:1–9.
12. Fung YC. Biomechanics: mechanical properties of living tissues. New York: Springer; 1993.
13. Theocaris PS, Sokolis DP. Invariant elastic constants and eigentensors of orthorhombic, tetragonal, hexagonal and cubic crystalline media. Acta Crystallogr A 2000;56:319–31.
14. Robicsek F, Thubrikar MJ. Role of sinus wall compliance in aortic leaflet function. Am J Cardiol 1999;84:944–6.
15. Missirlis YF, Chong M. Aortic valve mechanics—part I: material properties of natural porcine aortic valves. J Bioeng 1978;2:287–300.
16. Sauren AAHJ, van Hoyt MC, van Steenhoven AA, Veldpaus FE, Janssen JD. The mechanical properties of porcine aortic valve tissue. J Biomech 1983;16:327–37.
17. Ferraresi C, Bertetto AM, Mazza L, Maffiodo D, Franco W. One-dimensional experimental mechanical characterisation of porcine aortic root wall. Med Biol Eng Comput 1999;37:202–7.
18. Martin C, Pham T, Sun W. Significant differences in the material properties between aged human and porcine aortic tissues. Eur J Cardiothorac Surg 2011;40:28–34.
19. Azadani AL, Sam C, Matthews PB, et al. Comparison of mechanical properties of human ascending aorta and aortic sinuses. Ann Thorac Surg 2012;93:87–94.
20. Grande-Allen KJ, Cochran RP, Reinhall PG, Kunzelman KS. Re-creation of sinuses is important for sparing the aortic valve: a finite element study. J Thorac Cardiovasc Surg 2000;119:753–63.